Holographic Displacement Analysis Using Image-plane Techniques

Holographic-image-plane techniques are applied to measure displacement on diffuse surfaces. Results indicate that image-plane methods offer many distinct advantages over conventional holographic techniques

by J.A. Gilbert and G.A. Exner

ABSTRACT—This paper explores the potential of using image-plane holography as a tool in experimental mechanics to determine both 'in-plane' and 'out-of-plane' displacement components. Collimated-illumination and telecentric-imaging project displacement along common-sensitivity vectors over the full-field while white-light reconstruction helps to reduce speckle noise which allows high-density fringe gradients of good quality to be recorded. A holographic-image-plane multiplexing arrangement is developed to record different displacement components on a single hologram. Experiments are designed so that both reconstruction and optical filtering can be performed without a major modification of optical components. Displacements obtained from a centrally loaded circularly clamped plate are compared to their theoretical counterparts. Results show that image-plane techniques offer many distinct advantages over conventional methods for holographic analysis of displacement on diffuse surfaces.

List of Symbols

$\mathbf{d}$ = total displacement vector
$\mathbf{d}_\xi, \mathbf{d}_n$ = displacement projections
$\mathbf{e}_i$ = propagation vector
$\hat{\mathbf{e}}_i$ = unit vector in direction of propagation
$\mathbf{g}$ = sensitivity vector
$\mathbf{i}, \mathbf{j}, \mathbf{k}$ = basis of unit vectors
$\mathbf{n}$ = angle bisector direction
n, n_i, n_m = fringe-order numbers
u, v, w = scalar components of displacement
P, P' = point on the model surface
R = radius
X, Y, Z = Cartesian coordinates
α = sensitivity angle
δ = angular-phase change
λ = wavelength of laser light, 514.5 nm
ξ = coordinate direction

Introduction

The application of holographic interferometry to full-field displacement measurement is well known.[1-8] That is, if two holograms of an object in its undeformed and deformed states are superimposed on the same photographic plate, an interference pattern results over the surface of the model which characterizes the displacement initiated between exposures.

This paper explores the potential of using image-plane holography as a tool in experimental mechanics. The method is first applied to determine in-plane and out-of-plane displacement components for a flat surface. Analytical arguments are then formulated for a more general displacement separation to eliminate the need for using two separate experimental setups. A holographic-image-plane multiplexing arrangement is proposed which allows different displacement components to be recorded on a single hologram, each of which can be individually reconstructed in white light. This modified setup is designed so that both reconstruction and optical filtering can be performed without a major modification of optical components.

In all cases, experimental results are compared to their theoretical counterparts. The overall conclusion of the paper is that image-plane techniques offer many distinct advantages over the more conventional methods which are currently being used for the holographic analysis of displacement on diffuse surfaces.

Image-plane Holography

Image-plane holography has been documented in the literature;[9-14] however, its use as a tool for holographic interferometry is a relatively new concept in experimental mechanics.[15]

An image-plane hologram is one in which the image of an object, or the object itself, is located near the hologram recording plane. In practice, the most convenient way to satisfy this condition is to place an imaging system between the object and the photographic plate. This can be accomplished with either a simple lens or a complicated arrangement consisting of multiple lenses and apertures for advantages of magnification and/or increases in the depth of field.

A unique feature of the image-plane hologram is that it can be reconstructed in white light. That is, the coherence requirement on the reconstruction source is decreased as a consequence of the apparent proximity of the object to the photographic plate. When the developed hologram is illuminated with a white-light source, a real image of the

J.A. Gilbert and G.A. Exner are Assistant Professor and Graduate Student, respectively, Department of Mechanics, University of Wisconsin—Milwaukee, Milwaukee, WI 53201.

Paper was presented at 1977 SESA Spring Meeting held in Dallas, TX on May 15-20.

Original manuscript submitted: July 9, 1977. Final version received: February 3, 1978.

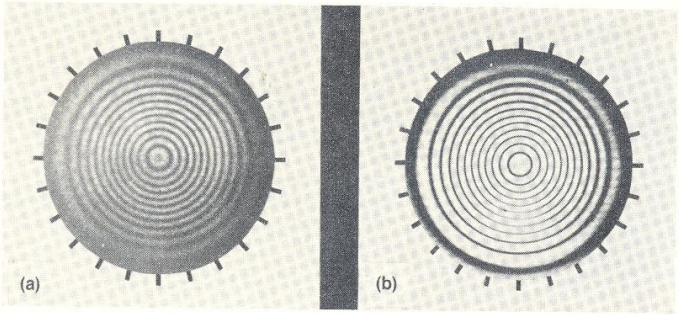

Fig. 1—Comparison of reconstructions taken from an image-plane hologram of the deflection pattern for a centrally loaded circularly clamped plate. (a) Laser-light reconstruction; (b) white-light reconstruction

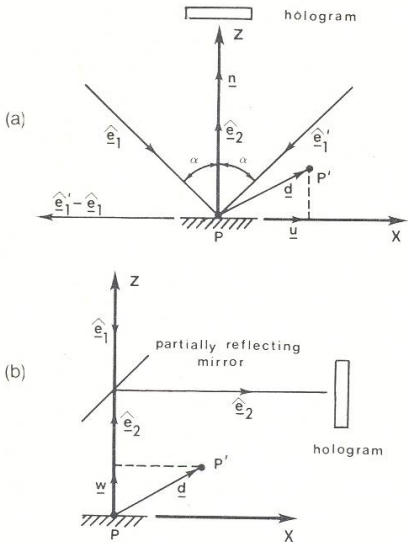

Fig. 2—Vector diagram for determining displacement. (a) In-plane displacement, u; (b) out-of-plane displacement, w

object can be viewed and/or recorded along the optical axis of the original imaging system by reversing the reference beam through the hologram. Optical inhomogeneities in the photographic plate have little effect on the real image and the reconstruction appears relatively sharp. The latter is extremely important for interferometric applications.

When a diffuse surface is illuminated with a laser, it appears speckled as a result of multiple interference of light bouncing from different parts of the surface. This speckle noise, which is also inherent in the laser-light reconstruction of double-exposed holograms, often makes it difficult to record high-density-fringe gradients of good quality. Image-plane holography and white-light reconstruction suppress this speckle noise. For example, Fig. 1 shows two reconstructions of the deflection pattern for a centrally loaded circularly clamped plate taken from an image-plane hologram. Identical recording mechanisms were used to photograph these reconstructions; however, Fig. 1(a) shows the hologram reconstructed in laser light, while Fig. 1(b) shows the same hologram reconstructed in white light. This improvement in fringe quality was the major reason for conducting the following feasibility study to determine whether or not image-plane techniques offer any other advantages over conventional holographic methods for displacement analysis in experimental mechanics.

Displacement Analysis—Initial Study

Consider a point on a diffuse surface which is illuminated with laser light along propagation vector $\mathbf{e}_1$ and observed along a propagation vector $\mathbf{e}_2$, usually taken to a point on the hologram. The fringe pattern which is observed upon double exposure of the photographic plate can be related to the displacement of the point between exposures.[16] That is, the governing equation for the displacement-fringe pattern reconstructed from a hologram of a diffuse surface is,

$$\delta = -(\mathbf{e}_1 - \mathbf{e}_2) \cdot \mathbf{d} \tag{1}$$

where δ is the angular phase change experienced by the point going through the displacement $\mathbf{d}$. Equation (1) holds for each model point and displacement fringes are observed when δ is an integer multiple of 2π. Introducing the wave number to convert eq (1) from angular to linear phase, one obtains,

$$n\lambda = -(\hat{\mathbf{e}}_1 - \hat{\mathbf{e}}_2) \cdot \mathbf{d} = \mathbf{g} \cdot \mathbf{d} \tag{2}$$

where n is the fringe order number, λ is the wavelength of the incident light, and $\hat{\mathbf{e}}_1$ and $\hat{\mathbf{e}}_2$ are unit vectors in the direction of illumination and observation, respectively. The vector $\mathbf{g}$ is often referred to as a sensitivity vector.

In general, the propagation vectors $\mathbf{e}_1$ and $\mathbf{e}_2$ change on a point-per-point basis and the displacement is projected along a different sensitivity vector for each model point. Ideally, one would like to see $\mathbf{g}$ remain constant over the full-field so that the fringe pattern characterized by eq (2) represents a single component of displacement. In general, this is not possible with conventional holographic techniques. The illumination may be collimated resulting in a constant vector $\mathbf{e}_1$; however, the observation of the model surface through the hologram creates a perspective effect which varies $\mathbf{e}_2$. Image-plane recording of the displacement field with a telecentric system,[17-19] consisting of two plano-convex lenses placed two focal distances apart, can be used to eliminate this problem. When large focal-distance lenses are used in the investigation and an adjustable aperture centrally located between the lenses is kept small, the object is effectively viewed from

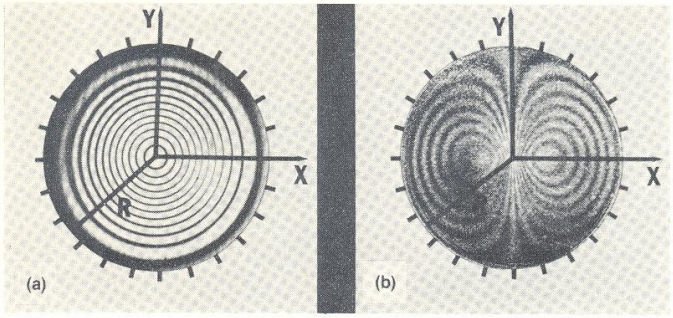

Fig. 3—Experimental results: displacement components for a centrally loaded circularly clamped plate. (a) Out-of-plane displacement, w. Each fringe corresponds to a displacement increment of 2.54×10^{-5} cm; (b) in-plane displacement, u. Each fringe corresponds to a displacement increment of 3.56×10^{-5} cm

infinity.[20] We found that 500-mm lenses and a 19-mm aperture were adequate to satisfy these conditions so that, for all intents and purposes, each model point was viewed as if its propagation vector $\mathbf{e}_2$ was parallel to the optical axis of the system. Therefore, for a collimated illumination and telecentric viewing, the sensitivity vector $\mathbf{g}$ remains constant over the full field and eq (2) is indicative of a single-displacement component.

Equations (1) and/or (2) can be modified to uniquely determine the in-plane and out-of-plane displacement components for a flat surface.

Figure 2(a) illustrates the basis for the holographic-moiré technique.[21] Two equally intense, collimated object beams given by $\hat{\mathbf{e}}_1$ and $\hat{\mathbf{e}}_1'$, respectively, illuminate a flat surface at equal angles α with respect to the surface normal $\mathbf{n}$. Laser light diffuses off the model to the hologram along vector $\hat{\mathbf{e}}_2$. A photographic plate is used to record the undeformed surface along with the reference-beam wavefront. The model is loaded and a second exposure is taken which superimposes the undeformed and deformed model states. Two double-exposure holograms are recorded, one due to each object beam. During reconstruction, two different interference fringe patterns are observed which are slightly displaced with respect to one another. That is, the displacement vector is projected along two different sensitivity directions. For $\hat{\mathbf{e}}_1$ and $\hat{\mathbf{e}}_2$, eq (2) takes the form,

$$n_1\lambda = -(\hat{\mathbf{e}}_1 - \hat{\mathbf{e}}_2) \cdot \mathbf{d} \tag{3}$$

Similarly, for $\hat{\mathbf{e}}_1'$ and $\hat{\mathbf{e}}_2$,

$$n_2\lambda = -(\hat{\mathbf{e}}_1' - \hat{\mathbf{e}}_2) \cdot \mathbf{d} \tag{4}$$

The intersection of these two displacement-fringe patterns gives rise to a moiré pattern whose parametrical equation is given by subtracting eq (3) from eq (4). That is,

$$(n_2 - n_1)\lambda = n_m\lambda = (\hat{\mathbf{e}}_1 - \hat{\mathbf{e}}_1') \cdot \mathbf{d} \tag{5}$$

where n_m is the moiré-fringe order number.

If unit vectors $(\mathbf{i},\mathbf{j},\mathbf{k})$ correspond to (X,Y,Z) in Fig. 2, then,

$$\hat{\mathbf{e}}_1 = \sin\alpha\,\mathbf{i} - \cos\alpha\,\mathbf{k} \tag{6}$$

and

$$\hat{\mathbf{e}}_1' = -\sin\alpha\,\mathbf{i} - \cos\alpha\,\mathbf{k} \tag{7}$$

where α is often referred to as a sensitivity angle. Furthermore, assuming that (u,v,w) are the displacement projections along (X,Y,Z), respectively, we can substitute eqs (6) and (7) into eq (5) to obtain,

$$u = \frac{n_m\lambda}{2\sin\alpha} \tag{8}$$

The displacement vector is projected onto the surface of the model, parallel to the X axis. Equation (5) indicates that the pattern for u is independent of the observation vector $\hat{\mathbf{e}}_2$. Therefore, the only requirement for eq (8) to be valid over the full field is that the dual-beam illumination is collimated. That is, image-plane techniques which incorporate a telecentric system are not necessary for in-plane displacement analysis.

It is evident from eq (2), however, that if the displacement $\mathbf{d}$ is to be projected normal to the surface of the model, $(\hat{\mathbf{e}}_1 - \hat{\mathbf{e}}_2)$ must be parallel to that normal for each model point. This situation can be satisfied with a normal illumination and a normal observation as shown in Fig. 2(b). In this case,

$$\hat{\mathbf{e}}_1 = -\mathbf{k} \tag{9}$$

and

$$\hat{\mathbf{e}}_2 = \mathbf{k} \tag{10}$$

Substituting eqs (9) and (10) into eq (2), one obtains,

$$w = \frac{n\lambda}{2} \tag{11}$$

Equation (11) depends upon both the illumination and observation of the surface. Therefore, a collimated illumination and a telecentric imaging system are necessary for eq (11) to be exact over the full field, indicating that image-plane methods must be used to holographically obtain full-field deflection patterns.

Experimental—Initial Study

A 12.7-cm-diam, 0.32-cm-thick plexiglass disk was painted flat white and sandwiched between a retaining plate and a steel frame to provide the centrally loaded circularly clamped plate used to illustrate the techniques documented in the initial feasibility study. The inner lip of the retaining plate created the effective 7.62-cm-diam fixed-support condition. The model was centrally loaded with a micrometer located behind the model surface. A 0.79-cm ball provided the contact point.

In-plane and out-of-plane displacement components were obtained with experimental setups based on Figs. 2(a) and 2(b), respectively. Collimated illumination and telecentric imaging were used in both investigations. Holograms were reconstructed in white light. Figure 3(a) shows the out-of-plane displacement, w, corresponding to a maximum center deflection of 3.175×10^{-4} cm.

The in-plane white-light reconstruction was recorded and then optically filtered with a coherent light source to eliminate the holographic-component patterns from the moiré and to increase moiré-fringe contrast. Figure 3(b) shows the filtered in-plane displacement component, u, corresponding to α equal to 45 deg and a midspan deflection of 5.08×10^{-3} cm. Figures 4 and 5 provide the theoretical and experimental comparisons for the respective displacement components where the theoretical curves are based on deflections due to bending stresses only.[22]

A dual-beam illumination parallel to the YZ plane with angle bisector along Z could have been used to obtain the v displacement component with the holographic-moiré technique; however, in view of the symmetry of the problem chosen to illustrate the method, the v pattern is analogous to the u pattern rotated through 90 deg.

Discussion

Techniques for determining the in-plane and out-of-plane displacement components for a centrally loaded circularly clamped plate using image-plane holography have been demonstrated. Analytical arguments indicated that image-plane holography is a must for full-field-deflection measurement. The out-of-plane reconstruction showed that the speckle noise, ordinarily inherent in laser-reconstructed holograms, was significantly reduced with white-light reconstruction. Also, high-density fringe gradients of good quality were recorded with a white-light reconstruction in the in-plane investigation. This gave rise to better diffraction efficiency during the optical filtering process, resulting in an improved filtered output.

The need to use more than one experimental setup to completely determine the Cartesian components of displacement, however, was an obvious drawback to the method. The model had to be loaded in each setup to determine the corresponding displacement projections.

The following study circumvents this drawback by combining the two setups used in the previous investigation into a single holographic-image-plane multiplexing arrangement. Different displacement components are recorded on a single hologram, each of which can be individually reconstructed in white light. The experimental setup is designed so that both reconstruction and optical filtering can be performed without a major modification of optical components.

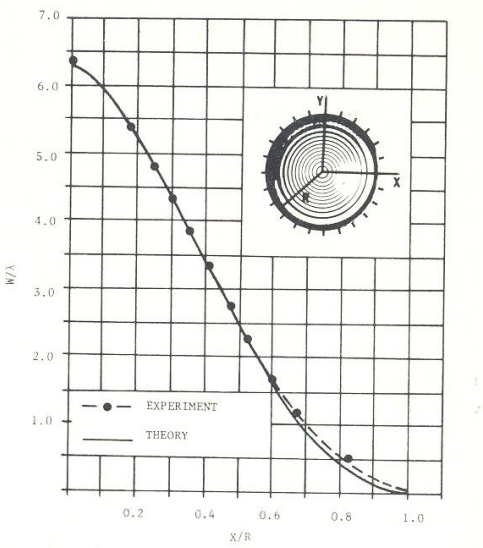

Fig. 4—Theoretical and experimental out-of-plane displacement along the radial center line of a centrally loaded circularly clamped plate. λ = 514.5 nm

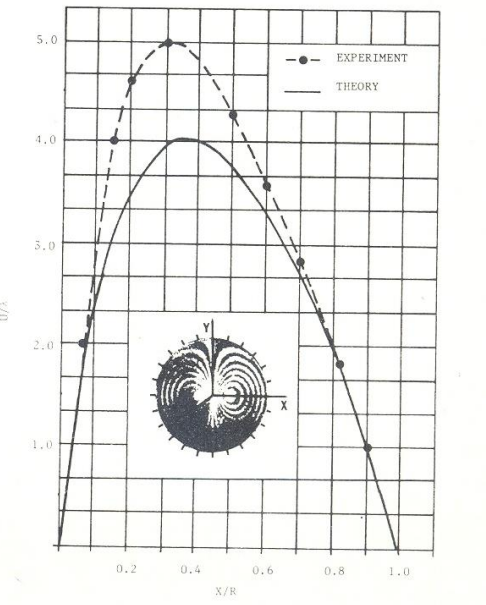

Fig. 5—Theoretical and experimental in-plane displacement along the radial center line of a centrally loaded circularly clamped plate. λ = 514.5 nm

The Method—Displacement Analysis

A point on the surface shown in Fig. 6 is illuminated with two collimated beams corresponding to the propagation vectors $\mathbf{e}_1$ and $\mathbf{e}_1'$, respectively. The observation direction is given by the propagation vector $\mathbf{e}_2$ and the diffused wavefronts from P are imaged on or near the photographic plate with a telecentric imaging system. (u, v, w) are the displacement projections along (X, Y, Z), respectively.

Let us assume that the illuminations are collimated and that a telecentric imaging system with large-focal-distance lenses and small aperture is used to record the holograms.

The normal illumination and the normal observation given by the unit vectors $\hat{\mathbf{e}}_1$ and $\hat{\mathbf{e}}_2$, respectively, produce a displacement-fringe pattern characterized by

$$w = \frac{n_1 \lambda}{2} \tag{12}$$

where n_1 is the fringe-order number.

The illumination vector $\hat{\mathbf{e}}_1'$ and the observation vector $\hat{\mathbf{e}}_2$ project the displacement along their angle bisector $\mathbf{n}$. This projection is labeled $\mathbf{d}_n$ on Fig. 6. From eq (2), we have

$$n_2 \lambda = -(\hat{\mathbf{e}}_1' - \hat{\mathbf{e}}_2) \cdot \mathbf{d} \tag{13}$$

where n_2 is the displacement-fringe-order number, and

$$\hat{\mathbf{e}}_1' = -\sin\alpha\,\mathbf{i} - \cos\alpha\,\mathbf{k} \tag{14}$$

Furthermore,

$$\hat{\mathbf{e}}_2 = \mathbf{k} \tag{15}$$

Substituting eqs (14) and (15) into eq (13), one obtains

$$n_2 \lambda = u \sin 2\alpha + w(\cos 2\alpha + 1) \tag{16}$$

Equation (16) is a linear combination of the u and w Cartesian-displacement components.

The displacement patterns corresponding to eqs (12) and (16), characterized by fringes assigned parameters n_1 and n_2, respectively, can also superimpose to form a moiré which is indicative of the displacement projected into a direction perpendicular to the angle bisector of the illumination vectors $\hat{\mathbf{e}}_1$ and $\hat{\mathbf{e}}_1'$. This so-called holographic-moiré technique is described in detail in Ref. 21 and has been applied to curved surfaces.[23] In Fig. 6, the displacement projected along ξ is referred to as $\mathbf{d}_\xi$. The equation governing this pattern is

$$(n_2 - n_1)\lambda = n_m \lambda = (\hat{\mathbf{e}}_1 - \hat{\mathbf{e}}_1') \cdot \mathbf{d} \tag{17}$$

where n_m is the moiré-fringe order number, and

$$\hat{\mathbf{e}}_1 = -\mathbf{k} \tag{18}$$

Furthermore,

$$\hat{\mathbf{e}}_1' = -\sin 2\alpha\,\mathbf{i} - \cos 2\alpha\,\mathbf{k} \tag{19}$$

Substituting eqs (18) and (19) into eq (17), one obtains

$$n_m \lambda = u \sin 2\alpha + w(\cos 2\alpha - 1) \tag{20}$$

Equation (20) is also a linear combination of the Cartesian displacement components u and w.

u and w can be uniquely determined when the fringe patterns corresponding to any two of eqs (12), (16) or (20) are analyzed. Similar arguments could be applied to a third noncoplanar collimated illumination to determine the remaining displacement component, v.

When the surface shown in Fig. 6 is flat and lies in the XY plane, u is referred to as the in-plane displacement and w is referred to as the out-of-plane displacement. In this case, it is desirable to capture $\mathbf{w}$ along with either of the other projections of $\mathbf{d}$; namely, $\mathbf{d}_\xi$ or $\mathbf{d}_n$. A unique solution can then be determined for u.

Consider capturing the out-of-plane displacement $\mathbf{w}$ along with the projected displacement $\mathbf{d}_n$. Substituting eq (12) into eq (16) and solving for u, we have

$$u = \frac{\lambda\{2n_m - n_1(\cos 2\alpha + 1)\}}{2 \sin 2\alpha} \tag{21}$$

When $\mathbf{w}$ is captured along with the projection $\mathbf{d}_\xi$, eq (12) can be substituted into eq (20), and

$$u = \frac{\lambda\{2n_m - n_1(\cos 2\alpha - 1)\}}{2 \sin 2\alpha} \tag{22}$$

Either eq (21) or (22) can be used to determine u.

Experimental

To demonstrate the proposed technique, a maximum center deflection of 1.27×10^{-3} cm was initiated to the centrally loaded circularly clamped plate previously described. The angle 2α was chosen to be 45 deg.

Displacement projections corresponding to eqs (12) and (20) were recorded on the same hologram with the experimental setup shown in Fig. 7. Two collimated object beams illuminated the model. The normal illumination and observation recorded the out-of-plane displacement $\mathbf{w}$, while the dual-beam illumination gave rise to a holographic-moiré pattern.

In order to multiplex the photographic plate, the collimated reference beam shown in Fig. 7 was divided

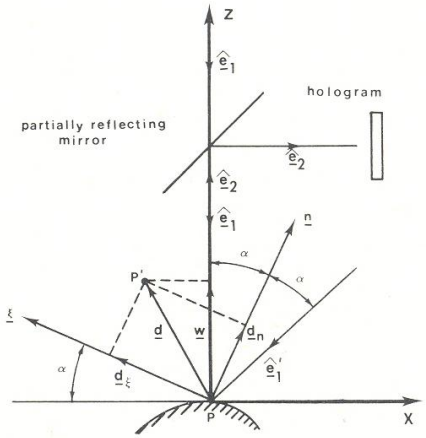

Fig. 6—Vector diagram for experimentally determining more than one projection of displacement on a single hologram

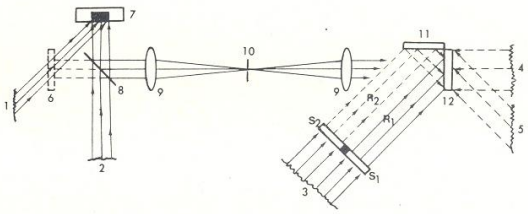

1. oblique object beam
2. normal object beam
3. reference beam
4. optical-filtering source
5. white-light source
6. removable diffusing glass
7. model
8. partially reflecting mirror
9. lens
10. adjustable aperture
11. front-surface mirror
12. hologram

Fig. 7—Experimental setup for determining two displacement components from a single hologram

into two parts, R_1 and R_2, with a double-shutter system S_1 and S_2. When recording the out-of-plane displacement, only S_1 was left open to expose the hologram to R_1 and the normal illumination. The holographic-moiré pattern was recorded with only S_2 open, exposing the hologram to R_2 and the dual illumination. Reference beam R_2 was reflected off a front-surface mirror so that R_1 and R_2 subtended different angles to the photographic plate. Each pattern could then be individually reconstructed with a collimated-white-light source at the appropriate reconstruction angle.

The experimental setup has some other unique properties. One advantage of such an arrangement is that the reference-object ratio can be controlled quite easily by changing the adjustable aperture of the lens system. Reconstruction is also possible with the telecentric imaging system. When the hologram is illuminated at the proper reconstruction angle with a collimated-white-light source, a real image forms on the model surface and, behind the partially reflecting mirror, along the optical axis of the system. Figure 8 illustrates this phenomenon and Fig. 9(a) shows the white-light reconstruction of the w displacement taken from a negative placed at the position of the diffusing glass shown in Figs. 7 and 8. Note that real-time displacement fringes could have been observed directly on the model surface if only the undeformed model state was recorded and reconstructed in the manner shown.

Incorporating reconstruction into the experimental setup allows the process to be performed without a major modification of optical components. It should be noted that the small aperture used in generating the image-plane holograms restricts the frequency band-pass of the telecentric imaging system, making the reconstruction process more critical. That is, even if an image-plane hologram is illuminated with collimated white light at the appropriate reconstruction angle, the corresponding image may be only partially reconstructed or appear multicolored when the imaging system used for recording the hologram is not used for reconstruction. When the real image is reconstructed with the generating-lens system, it is fully reconstructed and is monochromatic. Errors due to lens aberration are also minimized.

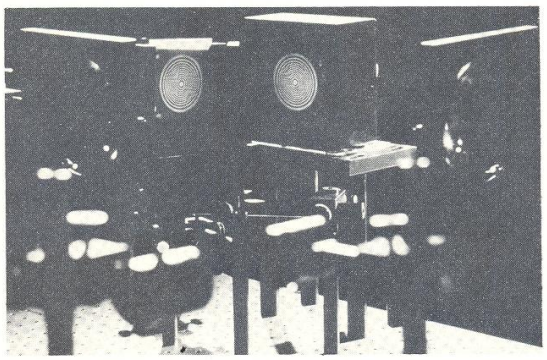

Fig. 8—A reconstructed image is simultaneously projected onto the model surface and the diffusing glass

The holographic-moiré pattern was reconstructed as described above; however, in this case, the moiré was captured along with its component patterns. Optical filtering was performed with the telecentric imaging system included in the experimental setup in order to sharpen fringe contrast and to eliminate the component patterns from the moiré. The unfiltered image obtained from the white-light reconstruction process was placed in the position of the hologram and an expanded, collimated laser beam, directed along the optical axis, illuminated this input from behind the plate. Note that this process required a separate illumination system also depicted in Fig. 7. A diffraction pattern was observed at the position of the aperture in the telecentric system and an appropriate stop positioned in this plane allowed a filtered, real image to be captured along the optical axis of the system on the diffusing glass located behind the partially reflecting mirror. The filtered holographic-moiré pattern for the centrally loaded circularly clamped plate is shown in Fig. 9(b).

The patterns shown in Fig. 9 were analyzed to determine the Cartesian displacement components given by eqs (12) and (22). A comparison of these experimental results with theoretical expressions based on displacements due to bending stresses only are shown in Figs. 10 and 11.

Errors were partially attributed to the model. Although the displacement-component patterns appear nearly 'symmetrical', the clamped condition was probably violated at the expected points of constraint, resulting in a plate with an effective diameter slightly larger than that used for theoretical comparison.

Conclusion

This paper has shown that image-plane holography can be used as an effective tool in experimental mechanics to determine 'in-plane' and 'out-of-plane' displacement com-

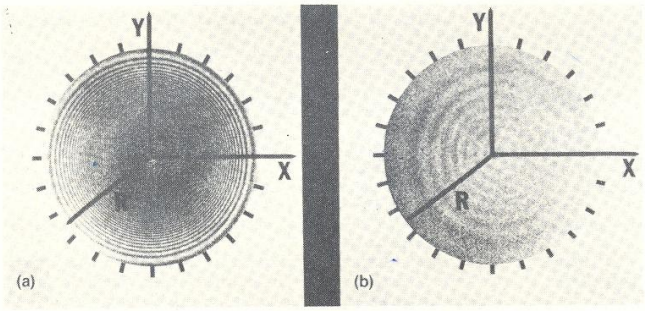

Fig. 9—Experimental results from the multiplexing technique. (a) Out-of-plane displacement, w; (b) Filtered moiré pattern of d_ξ

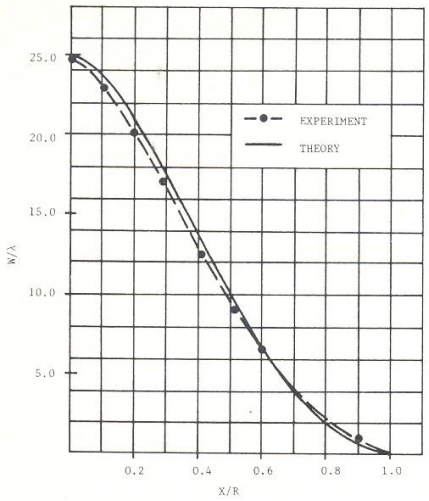

Fig. 10—Theoretical and experimental out-of-plane displacement along the radial center line of a centrally loaded circularly clamped plate. λ = 514.5 nm

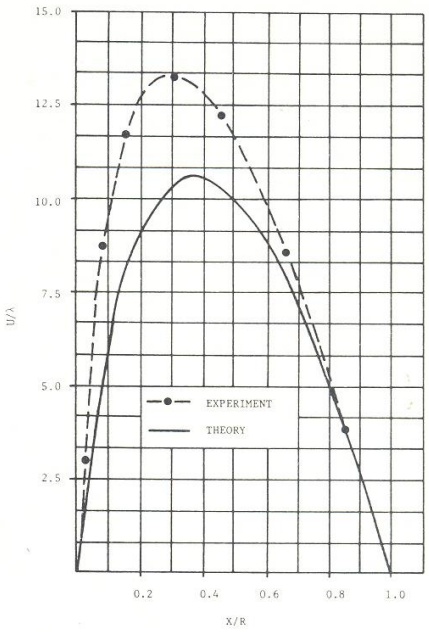

Fig. 11—Theoretical and experimental in-plane displacement along the radial center line of a centrally loaded circularly clamped plate. λ = 514.4 nm

ponents. Analytical arguments indicated that image-plane holography is a must for full-field deflection measurement. Speckle noise inherent in laser-light reconstruction was suppressed with white-light illumination of the image-plane holograms generated throughout the study. This allowed high-density fringe gradients of good quality to be recorded for displacement output or as input to an optical filtering system. A holographic multiplexing technique for the image-plane method has been established. Telecentric imaging was incorporated into an experimental setup to allow both reconstruction and optical filtering to be performed without a major modification of optical components. Image-plane holograms were reconstructed with the generating lens system resulting in a fully reconstructed and monochromatic real image in which lens aberrations were minimized. This arrangement had the added advantage that the reference-object ratio could be controlled quite easily by changing the adjustable aperture of the system as in normal photography. In short, it has been demonstrated that image-plane methods offer many distinct advantages over conventional holographic techniques.

References

1. *Horman, M.H., "Application of Wavefront Reconstruction to Interferometry," Appl. Opt.,* **4** *(1965).*

2. *Hildebrand, B.P. and Haines, K.A., "Surface-Deformation Measurement Using Wavefront Reconstruction Techniques," Appl. Opt.,* **5** *(1966).*

3. *Stetson, K.A., "The Argument of the Fringe Function in Hologram Interferometry of General Deformations," Optik,* **33** *(1970).*

4. *Sampson, R.C., "Holographic-interferometry Applications in Experimental Mechanics,"* EXPERIMENTAL MECHANICS, **10** *(8), 313-320 (Aug. 1970).*

5. *Robertson, E.R. and Harvey, J.M., The Engineering Uses of Holography, Cambridge Univ. Press, London (1970).*

6. *Shibayama, K. and Uchiyama, H., "Measurement of Three-Dimensional Displacements by Holographic Interferometry," Appl. Opt.,* **10** *(1970).*

7. *Dhir, S.K. and Sikora, J.P., "An Improved Method for Obtaining the General-displacement Field from a Holographic Interferogram,"* EXPERIMENTAL MECHANICS, **12** *(7), 323-327 (Jul. 1972).*

8. *Sciammarella, C.S. and Gilbert, J.A., "Strain Analysis of a Disk Subjected to Diametral Compression by Means of Holographic Interferometry," Appl. Opt.,* **12** *(1973).*

9. *Stroke, G.W., "White-Light Reconstruction of Holographic Images Using Transmission Holograms Recorded with Conventionally-Focused Images and 'In-Line' Background," Phys. Letters,* **23** *(1966).*

10. *Rosen, L., "Focused Image Holography with Extended Sources," Appl. Phys. Letters,* **9** *(1966).*

11. *Rosen, L. and Clark, W., "Film Plane Holograms Without External Source Reference Beams," Appl. Phys. Letters,* **10** *(1967).*

12. *Brandt, G.B. and Rigler, A.K., "Reflection Holograms of Focused Images," Phys. Letters,* **2** *(1967).*

13. *Brandt, G.B., "Image Plane Holography," Appl. Opt.,* **8** *(1969).*

14. *Leith, E.N., "White-Light Holograms," Scientific American,* **10** *(1976).*

15. *Maddux, G.E., Photomechanics Facility Technical Report, 2nd Ed., Air Force Flight Dynamics Laboratory (1976).*

16. *Sollid, J.E., "Holographic Interferometry Applied to Measurements of Small Static Displacements of Diffusely Reflecting Surfaces," Appl. Opt.,* **8** *(1969).*

17. *Nabelek, B., "Some Properties of Telecentric Systems," Optik,* **25** *(1967).*

18. *Walles, S., "Holographic Interferometry with Collimated Illumination and Telecentric Observation," Arkiv for Fysik,* **37** *(1968).*

19. *Luxmoore, A. and House, C., "Application of a Portable Telecentric Lens to Moiré Strain Measurements," J. Sci. Instr., (J. Phys. E.),* **5** *(1972).*

20. *Holister, G.S. and Watts, D., "Telecentric Systems for Moiré Analysis,"* EXPERIMENTAL MECHANICS, **10** *(1), 31-38 (Jan. 1970).*

21. *Sciammarella, C.A. and Gilbert, J.A., "A Holographic-moiré Technique to Obtain Separate Patterns for Components of Displacement,"* EXPERIMENTAL MECHANICS, **16** *(6), 215-220 (Jun. 1976).*

22. *Roark, R.J. and Young, W.C., Formulas for Stress and Strain, 5th Ed., McGraw-Hill (1975).*

23. *Gilbert, J.A., Sciammarella, C.A$_1$, and Chawla, S.K., "Extension to Three Dimensions of a Holographic-moiré Technique to Separate Patterns Corresponding to Components of Displacement,"* EXPERIMENTAL MECHANICS, **18** *(9), 321-327 (Sept. 1978).*